Article
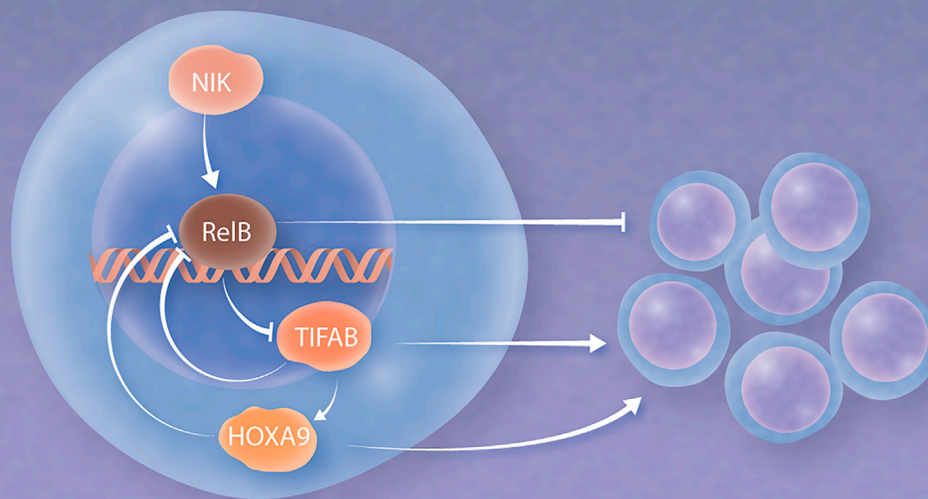
TIFAB accelerates MLL-AF9—Induced acute myeloid leukemia through upregulation of HOXA9

Jinming Zhao, Yan Xiu, Lin Fu, ..., Ulf Klein, Brendan F. Boyce, Chen Zhao

cxz545@case.edu

Highlights

RelB is essential for stabilization of NIK—induced AML suppression

TIFAB is a direct RelB target in MLL-AF9—induced AML

TIFAB accelerates MLL-AF9—induced AML via upregulation of HOXA9

Article

TIFAB accelerates MLL-AF9−Induced acute myeloid leukemia through upregulation of HOXA9

Jinming Zhao,[1,2,10] Yan Xiu,[1,3,10] Lin Fu,[2,10] Qianze Dong,[1,3] Nicholas Borcherding,[4] Yang Wang,[1] Qingchang Li,[2] Nilushi S. De Silva,[5] Ulf Klein,[6] Brendan F. Boyce,[7] and Chen Zhao[3,8,9,11,]*

SUMMARY

We previously showed stabilization of NIK−induced activation of NF-κB non-canonical signaling suppresses MLL-AF9−induced AML. In the current study, we demonstrate that deletion of NF-κB non-canonical RelB prevents the inhibitory effect of NIK stabilization in MLL-AF9 AML. Mechanistically, RelB suppresses its direct target, TIFAB, which is upregulated in human AML and correlates negatively with the survival of AML patients. Forced expression of TIFAB reverses NIK−induced impaired AML development through downregulation of RelB and upregulation of HOXA9. Consistent with upregulation of HOXA9, gene set enrichment analysis shows that forced expression of TIFAB blocks myeloid cell development, upregulates leukemia stem cell signature and induces similar gene expression patterns to those of HOXA9-MEIS1 and HOXA9-NUP98, and upregulates oxidative phosphorylation. Accordingly, forced expression of HOXA9 also largely releases the inhibitory impact of NIK stabilization via downregulation of RelB and upregulation of RelA. Our data suggest that NIK/RelB suppresses MLL-AF9−induced AML mainly through downregulation of TIFAB/HOXA9.

INTRODUCTION

Acute myeloid leukemia (AML) is an aggressive hematologic malignancy characterized by clonal proliferation of hematopoietic stem or progenitor cells (Khwaja et al., 2016; Pollyea and Jordan, 2017; Tallman et al., 2019). Despite decades of research, AML is still associated with high mortality (5-year survival rate <30%) and recurrence rates with limited treatment options (Dohner et al., 2017; Dombret and Gardin, 2016). AML is initiated and maintained by a small minority of self-renewing leukemia stem cells (LSCs), which are biologically distinct from bulk tumor, have differential sensitivity to chemotherapy, and are a major cause of therapy resistance and relapse (Jordan et al., 2006; Kreso and Dick, 2014; Mikkola et al., 2010).

Canonical nuclear factor κB (NF-κB) signaling is constitutively activated in AML stem cells and required for LSC self-renewal and positively correlates with resistance to therapy (Bosman et al., 2016; Gasparini et al., 2014; Guzman et al., 2007). Contrary to the role of canonical NF-κB signaling in AML, NF-κB-inducing kinase (NIK)-initiated non-canonical NF-κB signaling represses canonical signaling and suppresses MLL-AF9-induced AML (Xiu et al., 2018). However, whether non-canonical signaling is essential for NIK's inhibitory effect and is a downstream target of non-canonical signaling in AML are unclear.

TRAF-interacting protein with forkhead-associated domain B (TIFAB) is located in the commonly deleted region on chromosome 5q in myelodysplastic syndromes (MDSs) as well as AML (Niederkorn et al., 2020a). Loss of TIFAB impairs normal hematopoiesis through enhancing TLR4-TRAF6 signaling (Varney et al., 2015). In addition, it has been shown recently that in MLL-AF9 leukemia, deletion of TIFAB decreases leukemic cell function and development by increasing p53 signaling, and conversely, elevated TIFAB represses p53, increases leukemia progenitor function by increasing the activity of ubiquitin-specific peptidase 15 (USP15) ubiquitin hydrolase (Niederkorn et al., 2020b). However, given that TIFAB was initially identified as an NF-κB signaling inhibitor (Matsumura et al., 2009), its interaction with NF-κB signaling in AML and how TIFAB accelerates AML progression requires further study.

[1]Department of Pathology, Case Western Reserve University, Wolstein Research Building, Room 6503 2103 Cornell Road, Cleveland, OH 44106, USA

[2]Department of Pathology, China Medical University, 77 Puhe Road, Shenbei Xinqu, Shenyang, Liaoning Province, 110122, China

[3]Department of Pathology, Louis Stokes Veterans Affairs Medical Center, Cleveland, OH 44106, USA

[4]Department of Pathology and Immunology, Barnes-Jewish Hospital, Washington University in St Louis, MO 63110, USA

[5]Institut Curie, PSL Research University, INSERM U932, Paris, France

[6]Division of Haematology & Immunology, Leeds Institute of Medical Research at St. James, Leeds LS9 7TF, UK

[7]Department of Pathology and Laboratory Medicine, University of Rochester Medical Center, Rochester, NY 14642, USA

[8]Department of Pathology, University Hospitals Case Medical Center, Cleveland, OH 44106, USA

[9]Department of Pathology, Case Western Reserve University, Wolstein Research Building, Room 6523 2103 Cornell Road, Cleveland, OH 44106, USA

[10]These authors contributed equally

[11]Lead contact

*Correspondence: cxz545@case.edu

https://doi.org/10.1016/j.isci.2021.103425

Here, we demonstrate that non-canonical NF-κB RelB is required for NIK-induced suppression of MLL-AF9 leukemia, at least partially through downregulation of TIFAB, and TIFAB accelerates MLL-AF9 leukemia progression by negatively regulating RelB and positively upregulating HOXA9, a known critical regulator in AML.

RESULTS

RelB is essential for stabilization of NIK–induced impaired leukemogenesis

Our previous studies have shown that stabilization of NIK suppresses MLL-AF9-induced acute myeloid leukemia (AML) mainly through upregulation of RelB, which upregulates DNMT3A and downregulates MEF2C (suppresses and promotes AML, respectively), and repression of RelA (Xiu et al., 2018). However, the detailed underlying molecular mechanisms remain unknown. To determine if non-canonical signaling is essential for stabilization of NIK–induced impaired leukemogenesis, we generated NIK-stabilized MLL-AF9-induced AML cells in the absence of *Relb* using the newly established compound-mutant mouse, NIK^{flSTOP}Relb$^{fl/fl}$ERT2. Compared with NIK-stabilized [Tamoxifen(Tam)-treated NIK^{flstop}ERT2 mice, CaNIK] AML cells, deletion of *Relb* (Tam-treated NIK^{flstop}Relb$^{fl/fl}$ERT2 mice, CaNIKRelBKO) completely restored the reduced engraftment ability of NIK-stabilized AML cells (Figure 1A). Deletion of RelB was confirmed by immunoblotting and genotyping (Figure 1B and not shown).

Stabilization of NIK downregulates TIFAB, a direct target of non-canonical NF-κB signaling

To identify the RelB target that is responsible for suppression of MLL-AF9-induced AML, we focused on Tifab (TRAF-interacting protein with forkhead-associated domain B), which was downregulated in NIK stabilized MLL-AF9—induced AML (Xiu et al., 2018), and is involved in hematopoiesis, myelodysplastic syndrome and AML (Matsumura et al., 2009; Niederkorn et al., 2020a, 2020b; Varney et al., 2015). We confirmed that expression of TIFAB protein was downregulated in NIK-stabilized MLL-AF9 leukemia, and found its expression was largely restored in the absence of RelB (Figure 1B), suggesting that TIFAB is a downstream NIK-RelB target. Chromatin immunoprecipitation-PCR analysis showed that RelB directly bound two (F104 and F191) of three potential NF-κB binding sites in the *Tifab* promoter region (Figure 1C). In addition, overexpression of RelB, but not RelA, suppressed the expression of TIFAB protein in both murine (Figure 1D) and human MLL-AF9 leukemia cells (Figure 1E), further demonstrating that TIFAB is a direct RelB target in MLL-AF9 leukemia.

TIFAB accelerates MLL-AF9-induced AML

To investigate the cellular impact of TIFAB on AML, we compared proliferation and apoptosis between TIFAB- and vector-transduced cKit$^+$ MLL-AF9 leukemia cells. Cell counting, BrdU incorporation and Ki67 staining all showed that TIFAB significantly accelerated AML cell proliferation (Figures 2A–2C), whereas modestly inhibiting cell apoptosis (Figure 2D). TIFAB expression also upregulated the expression of CD117, an immature marker in MLL-AF9-induced AML, suggesting that TIFAB expression increased the frequency of leukemia stem/progenitor cells (Figure 2E). In addition, TIFAB expression increased leukemia cell colony formation *in vitro* and repopulation *in vivo*, and largely released the suppressive impact of NIK stabilization induced by 4-OHT (Figures 2F and 2G). Importantly, Tifab mRNA expression (GEPIA2 dataset) is significantly increased in AML patients compared with healthy controls (Figure 2H), and higher TIFAB expression is correlated with poorer overall survival (Figure 2I) in AML patients. Collectively, these data indicate that TIFAB accelerates AML cell proliferation and corroborated its function in AML, as reported recently (Niederkorn et al., 2020b).

TIFAB upregulates gene sets involved in LSC maintenance

To investigate the underlying molecular mechanism whereby TIFAB enhances leukemogenesis, we performed RNA-sequencing (RNA-seq) using FACS-sorted control or TIFAB-transduced leukemic stem cells (Lin$^{lo/-}$Sca1$^-$CD117$^+$CD16$^+$CD34$^+$) from mice with full-blown leukemia. Compared to control LSCs, TIFAB LSCs showed downregulation of genes related to myeloid differentiation (Cd14, Cd163, Mpo, Elane, Csf1r) and cell cycle inhibition (Cdkn2a), whereas upregulated genes related to maintenance of the LSC signature (*Six1, Msi2, Flt3,* and *Hoxa* gene families) (Calvo et al., 2000; Chu et al., 2019; Collins and Hess, 2016; Ito et al., 2010; Kennedy and Smith, 2020) (Figure 3A). The upregulation of FLT3 also contributes to TIFAB's leukemia-enhancing impact, given that FLT3 is commonly mutated (approximately one-third of newly diagnosed AML) and associated with increased relapse and inferior overall survival (Kennedy and Smith, 2020). The upregulation of *Hoxa* cluster genes was further validated by quantitative RT-PCR analysis (Figure 3B).
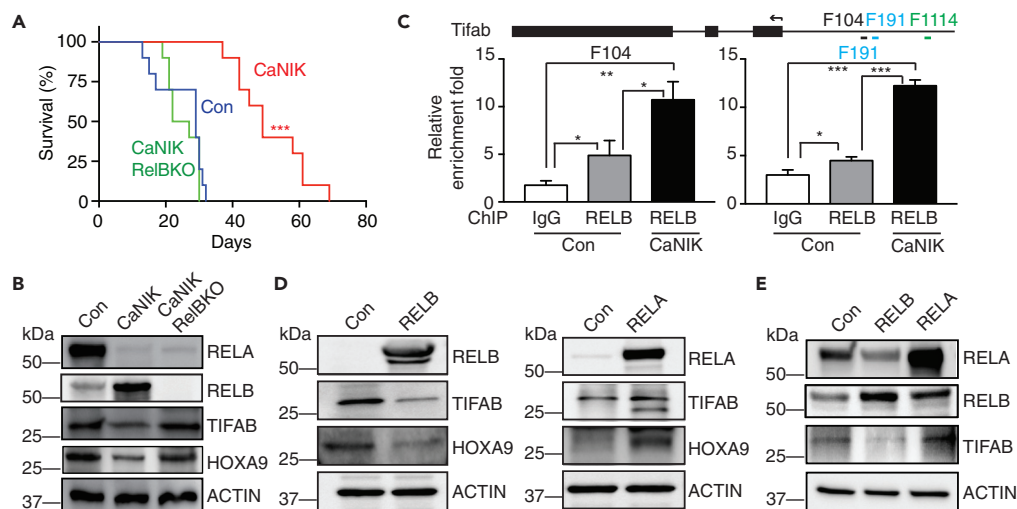
Figure 1. *Tifab* is a direct downstream target of RelB

(A) Survival curve of sublethally irradiated recipient mice receiving twenty thousand sorted leukemia stem/progenitor cells (LSPCs, defined as Lin⁻Sca1⁻CD117⁺ cells) from untreated MLL-AF9 NIKERT2 (**Con**, GFP-) or tamoxifen-treated MLL-AF9 NIKERT2 (**CaNIK**, GFP+) or tamoxifen-treated MLL-AF9 NIK^{flstop}Relb$^{fl/fl}$ERT2 (**CaNIKRelBKO**) leukemic mice (n = 10 in each group, two replicates). ***p < 0.001, log rank test.

(B) The expression of RELA, RELB, TIFAB and HOXA9 protein in full-blown Con, CaNIK or CaNIKRelBKO MLL-AF9 leukemia cells. Beta-actin was used as loading control. Shown are representative results of three independent experiments.

(C) Chromatin immunoprecipitation (ChIP) – quantitative polymerase chain reaction (qPCR) analysis of RELB binding sites in the *Tifab* promoter region. Upper, putative RELB binding sites F104, F191 and F114. Arrow marks transcriptional start site. Note, F114 binding site was tested previously and did not show RELB binding. Lower, sheared chromatin from Con or CaNIK MLL-AF9 leukemia cells were precipitated with RELB or immunoglobulin G (IgG) and followed by real-time PCR (Representative results of two independent experiments). Note that RELB binds both F104, and F191 sites. Data are represented as means ± SEM (standard error of mean). *p < 0.05; **p < 0.01; ***p < 0.001, t test.

(D) The expression of RELB, TIFAB, and HOXA9 protein in RELB-overexpressing MLL-AF9 leukemia cells (left) and the expression of RELA, TIFAB, and HOXA9 protein in RELA-overexpressing MLL-AF9 leukemia cells (right). Shown are representative results of three independent experiments and ACTIN was used as a loading control.

(E) The expression of RELB, RELA, and TIFAB protein in RELB-overexpressing or RELA-overexpressing NOMO-1 leukemia cells. Shown are representative results of two independent experiments and ACTIN was used as a loading control.

Consistent with downregulation of myeloid differentiation genes and upregulation of genes related to LSC signatures, gene set enrichment analysis (GSEA) showed that TIFAB downregulated genes related to myeloid cell development (Figure 3C) and genes that are reduced in LSCs (Figure 3D), respectively. Consistent with the upregulation of *Hoxa* gene expression, GSEA further revealed that TIFAB played a similar role as expression of Hoxa9-Meis1 (Figure 3E) and Hoxa9-NUP98 (Figure 3F). Importantly, TIFAB increased LSC oxidative phosphorylation, a critical process for maintenance of LSC activities (Farge et al., 2017; Lagadinou et al., 2013) (Figure 3G). Collectively, these data suggest that TIFAB enhances expression of genes involved in LSC maintenance and proliferation.

Overexpression of HOXA9 significantly releases stabilization of NIK-induced suppression of AML

Among the upregulated Hoxa family genes, Hoxa9 has been shown to play critical roles in different subtypes of AML, e.g., MLL-AF9-induced AML and AML with mutated NPM1 (Brunetti et al., 2018; Chen et al., 2019; Collins and Hess, 2016; Milne et al., 2002; Mulligan et al., 2007). We first validated the upregulation of HOXA9 proteins in TIFAB-transduced leukemia cells by Western Blotting (Figure 4A). We then examined the impact of forced expression of HOXA9 on stabilization of NIK-induced AML suppression. Like forced expression of TIFAB, which completely rescued NIK's inhibitory effect, overexpression of HOXA9 also largely released stabilization of the NIK-induced suppressive effect on colony formation and leukemia cell repopulation in mice (Figures 4B and 4C).
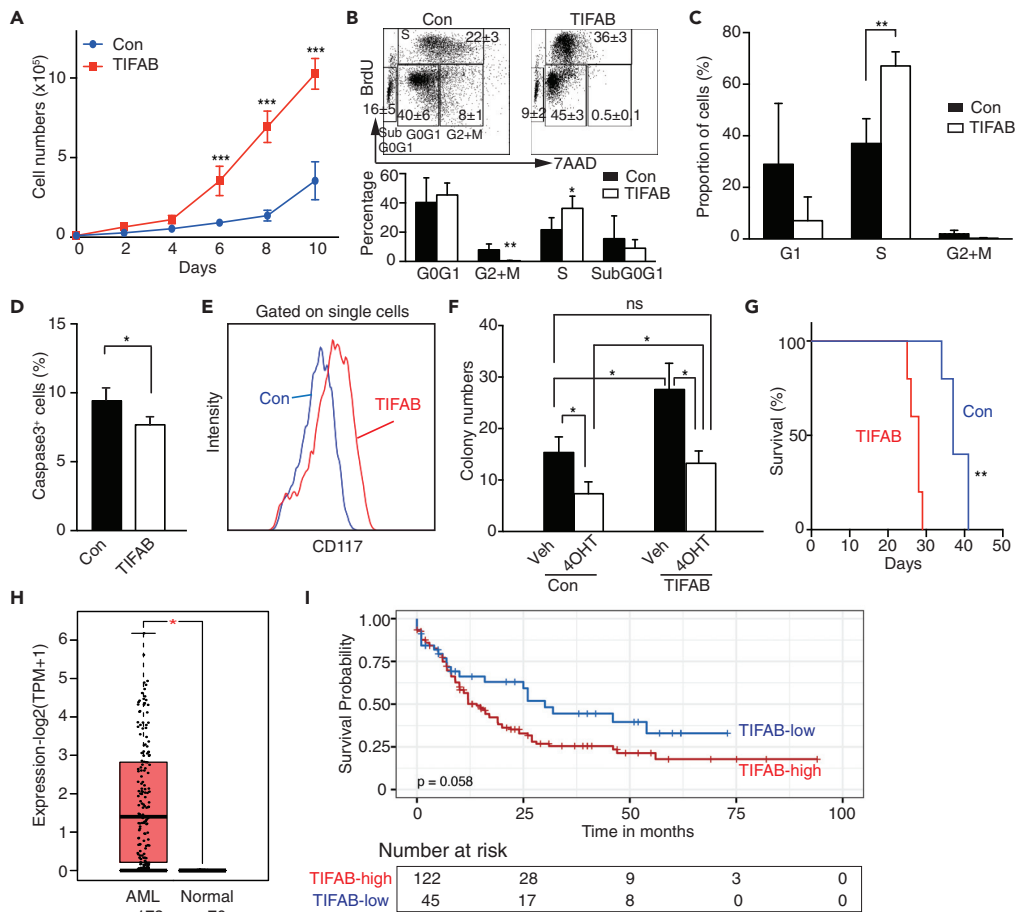
Figure 2. TIFAB promotes MLL-AF9 leukemic cell proliferation and accelerates MLL-AF9 leukemia expansion
in vivo

(A) Cell counting of vector (Con) or MLL-AF9 leukemia cells overexpressing TIFAB. 10
K vector or TIFAB-overexpressing leukemia cells were plated and counted every other day for 10 days. Data are represented as means $\pm$ SEM. ***p < 0.001, t test.

(B) Percentage of BrdU$^+$ Con or leukemia cells overexpressing TIFAB in different cycle phases. Data are represented as means $\pm$ SEM. **p < 0.01, t test.

(C) Percentage of Ki67$^+$ leukemia cells in Con or MLL-AF9 leukemia cells overexpressing TIFAB. Data are represented as means $\pm$ SEM. **p < 0.01, t test.

(D) Percentage of Caspase3$^+$ leukemia cells in Con or leukemia cells overexpressing TIFAB. Data are represented as means $\pm$ SEM. *p < 0.05, t test.

(E) Expression of immature marker CD117 in Con or leukemia cells overexpressing TIFAB.

(F) Colony numbers of Con or leukemia cells overexpressing TIFAB with or without 4-hydroxytamoxifen (4-OHT, 0.25 μM). Data are represented as means $\pm$ SEM. *p < 0.05, t test. A–F, representative results of at least three independent experiments.

(G) Survival curve of sublethally irradiated mice receiving TIFAB- or empty-vector (Con)-transduced MLL-AF9 leukemia cells (n = 5 each, representative results of two independent experiments). **p < 0.01, log rank test.

(H) Expression of *Tifab* mRNA in AML and normal controls. Data were extracted from GEPIA2 Database, which combines TCGA (the Cancer Genome Atlas) and GTEx (Genotype-Tissue Expression) data. The normal controls are unrelated normal bone marrow tissue in the TCGA and GTEx datasets. Data are represented as means $\pm$ SEM. *p < 0.05, t test.

(I) Higher expression of *Tifab* (TCGA database) correlates with a worse survival.

TIFAB was initially identified as a molecule that inhibits NF-κB signaling (Matsumura et al., 2009), and it has been reported that NF-κB is a major transcription factor required for HOXA9 downregulation (Trivedi et al., 2008). We hypothesized that TIFAB upregulates HOXA9 through inhibition of NF-κB signaling. In fact, we found that overexpression of TIFAB suppressed the expression of both RelA
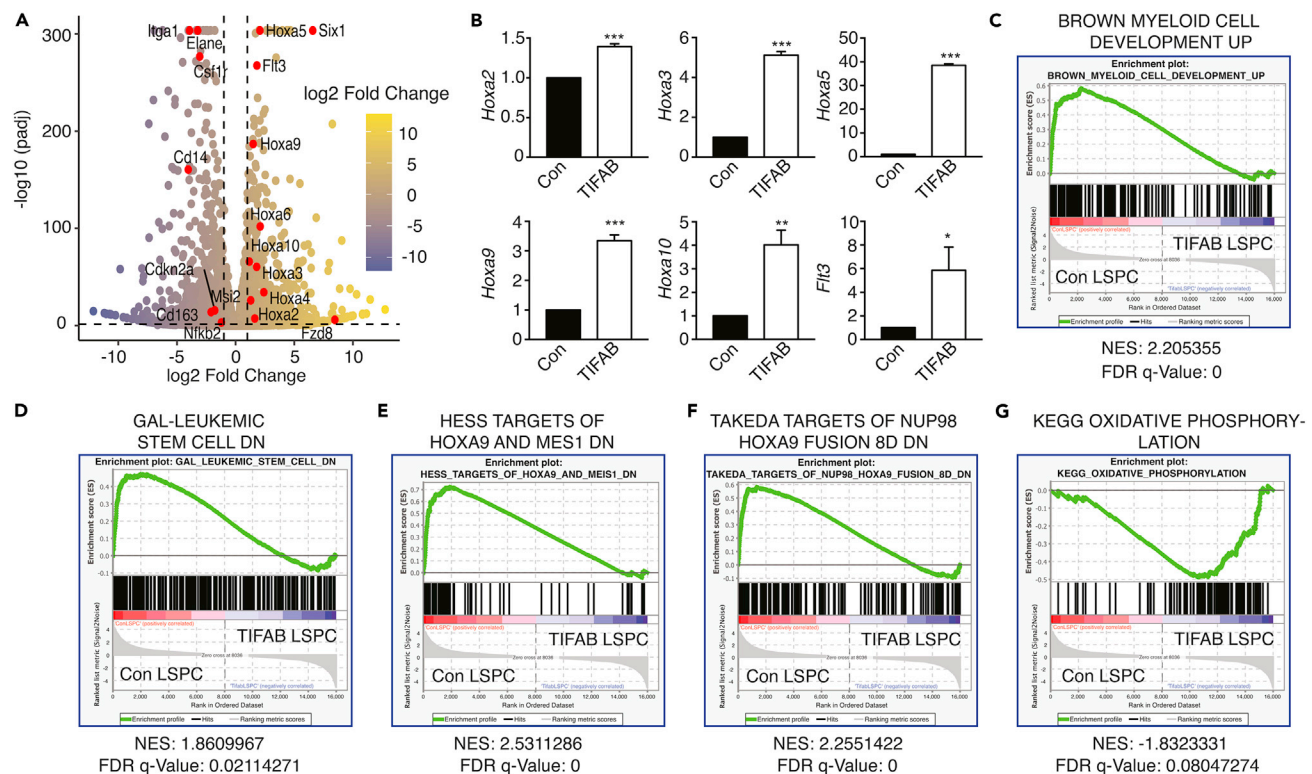
Figure 3. TIFAB upregulates Hoxa cluster genes in MLL-AF9 leukemia stem cells

(A) Volcano plot of genes up- and down-regulated in TIFAB-, compared with Vector-, transduced leukemia stem cells (defined as Lin$^-$Sca1$^-$cKit$^+$CD34$^+$CD16$^+$). Two biological replicates each. Note the upregulated *Hoxa* cluster genes.

(B) qPCR analysis of the expression of *Hoxa2*, *Hoxa3*, *Hoxa5*, *Hoxa9*, *Hoxa10*, and *Flt3* in vector- (Con) or TIFAB- expressing leukemia stem cells. Three replicates each, shown are representative results of three independent experiments. Data are represented as means ± SEM. *p < 0.05; **p < 0.01; ***p < 0.001, t test.

(C–G) Gene Set Enrichment Analysis (GSEA) of RNA-seq data of Con and TIFAB-overexpressing leukemia stem cells. C, downregulation of myeloid cell development gene set; D, upregulation of leukemia stem cell gene set (downregulation of genes reduced in leukemia stem cells); E, downregulation of the gene set that was reduced by HOXA9-MEIS1; F, downregulation of the gene set that was reduced by HOXA9-NUP98; and G, upregulation of oxidative phosphorylation by forced expression of TIFAB. FDR, false discovery rate. NES, normalized enrichment score.

and RelB proteins and also p53, as reported recently (Niederkorn et al., 2020b) (Figure 4D), while up-regulating expression of HOXA9 proteins (Figure 4A). Furthermore, RelA and RelB differentially regulated HOXA9 expression: RelA enhanced while RelB suppressed HOXA9 expression (Figure 1D). In addition, NIK stabilization-induced suppression of HOXA9 was RelB-dependent, because in the absence of RelB, HOXA9 expression levels returned to normal, as in control leukemia cells (Figure 1B). Interestingly, overexpression of HOXA9 downregulated the expression of RelB, while upregulating expression of RelA, and largely maintained the expression of TIFAB in NIK-stabilized leukemia cells (Figure 4E). Collectively, these results suggest canonical and non-canonical NF-κB signaling and HOXA9 positively and negatively regulate each other, respectively, and HOXA9 is a critical TIFAB downstream effector in MLL-AF9 leukemia.

DISCUSSION

In the current report, we have shown that RelB is essential for stabilization of NIK-induced impaired leukemogenesis, which further substantiates our previous conclusion that NIK suppresses AML through activation of NF-κB non-canonical signaling (Xiu et al., 2018). In addition, we identify TIFAB as a direct non-canonical signaling target that functions as an oncogene to accelerate AML progression and completely rescues stabilization of NIK-induced impaired leukemogenesis. Importantly, higher expression of TIFAB correlates to a poor overall survival in AML patients.
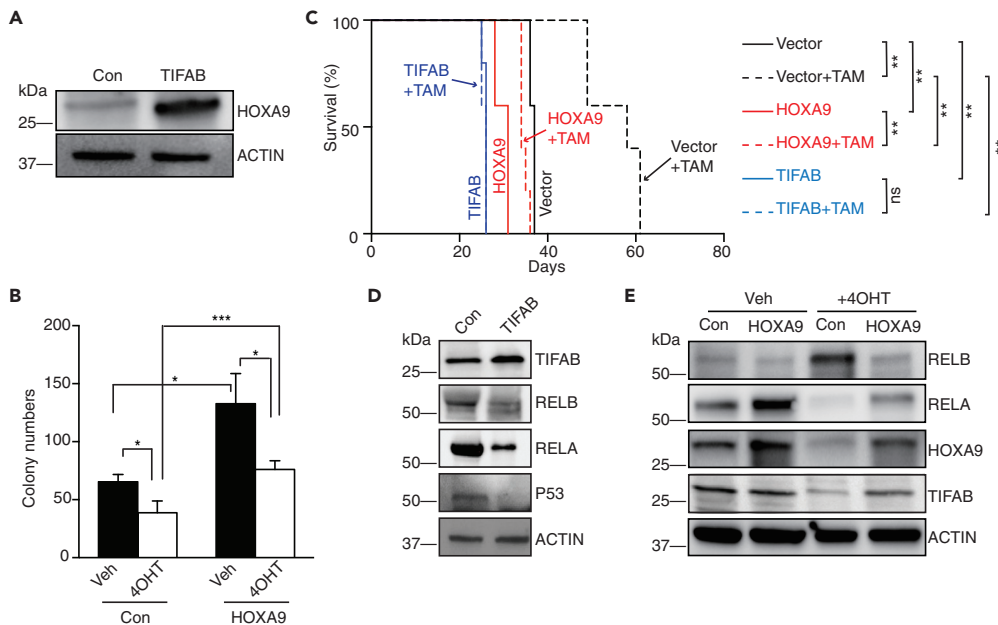
Figure 4. Forced expression of HOXA9 significantly releases the inhibitory effect of NIK stabilization

(A) HOXA9 protein expression in vector- (Con) or TIFAB-overexpressed MLL-AF9 leukemia cells. Beta-actin was used as loading control. Data shown are representative of three independent experiments.

(B) Number of colonies of vector- (Con) or HOXA9-overexpressing MLL-AF9 leukemia cells in the presence or absence of 4-OHT (n = 3). Shown are representative results of four independent experiments Data are represented as means ± SEM. *p < 0.05; ***p < 0.001, t test.

(C) Survival curve of sublethally irradiated recipient mice receiving vector-, TIFAB- or HOXA9-transduced MLL-AF9 leukemia cells (n = 5 in each group) in the presence or absence of 4-OHT. Shown are representative results of two independent experiments ns, no significance; **p < 0.01, log rank test.

(D) Expression of TIFAB, RELB, RELA, and P53 protein in vector- (Con) or TIFAB-overexpressing MLL-AF9 leukemia cells. Beta-actin was used as a loading control.

(E) Expression of NIK, RELB, RELA, and HOXA9 protein in vector- (Con) or HOXA9-overexpressing MLL-AF9 leukemia cells in the presence or absence of 4-OHT. D and E, data shown are representative of three independent experiments.

Consistent with binding of TIFAB to TRAF6 suppressing TRAF6-mediated TLR-NF-κB signaling (Matsumura et al., 2009), our data show that forced expression of TIFAB in MLL-AF9 leukemia cells suppresses the expression of RelB, indicating the existence of a negative feedback loop between RelB and TIFAB. Intriguingly, forced expression of TIFAB also suppresses the expression of RelA, a key player in NF-κB canonical signaling, which is constitutively activated in AML stem cells and is required for LSC self-renewal (Bosman et al., 2016; Gasparini et al., 2014; Guzman et al., 2007), this along with our previous data show that overexpression of RELA (in contrast overexpression of RELB) enhances MLL-AF9-induced AML, suggesting that TIFAB may activate additional oncogenic signaling, which will bypass the requirement of NF-κB canonical signaling.

Through RNA-sequencing analysis of the TIFAB-transduced and empty vector-transduced leukemia stem/progenitor cells, we show that TIFAB upregulates *Hoxa* cluster genes, including *Hoxa9*, which has been shown to play an important role in MLL-AF9 leukemia and other subtypes of AML (Brunetti et al., 2018; Collins and Hess, 2016). In contrast with upregulation of Hoxa9, TIFAB-transduced leukemia stem/progenitor cells display a similar gene expression pattern to those induced by Hoxa9-Meis1 and Hoxa9-NUP98. Furthermore, TIFAB-transduced leukemia stem/progenitor cells show increased oxidative phosphorylation, which is critical for LSC maintenance (Jordan, 2019). Importantly, forced expression of HOXA9 largely reversed stabilization of NIK-induced delayed leukemogenesis. Therefore, even though TIFAB suppresses the expression of RelA and RelB, upregulation of HOXA9 can compensate for the inhibition of NF-κB signaling.

Interestingly, forced expression of HOXA9 downregulates RelB, but in contrast to TIFAB, it upregulates RelA. The interaction of NF-κB and HOXA9 is complicated and context-dependent (Pai and Sukumar, 2020). For example, HOXA9 is a tumor suppressor in many solid malignancies, where it inhibits NF-κB signaling (Han et al., 2019). In endothelial cells, HOXA9 and NF-κB negatively regulate each other (Trivedi et al., 2008). In hematological neoplasms, HOXA9 is an oncogene and RELA has been shown to occupy the HOXA9 and MEIS1 promoters to regulate their expression (Kuo et al., 2013). The upregulation of RELA and downregulation of RELB (Figure 4E) suggest that HOXA9 differentially regulates canonical and non-canonical NF-κB pathways. Conversely, downregulation of HOXA9 by RelB and upregulation of HOXA9 by RelA (Figure 1D) suggest that non-canonical and canonical signaling differentially regulate Hoxa9 expression.

TIFAB has recently been shown to increase leukemia progenitor cell functions through regulation of ubiquitin-specific peptidase 15 ubiquitin hydrolase activity to repress p53 (Niederkorn et al., 2020b). Our report complements these previous studies and reveals a new function of TIFAB to regulate AML progression through a signaling cascade involving NIK-RELB-TIFAB-HOXA9. Targeting TIFAB directly or through stabilization of NIK may be an attractive therapeutic option to treat MLL-AF9 leukemia. It should be noted that given TIFAB is not a transcription factor, its regulation of the HOXA gene program is most likely indirect, via regulation of NF-κB signaling. In addition, a recent report (Muto et al., 2020) demonstrated that in response to inflammation, HSPCs (hematopoietic stem/progenitor cells) in MDS (myelodysplastic syndrome) patients and mice switch from canonical to noncanonical NF-κB signaling, suggesting that non-canonical signaling is critical for MDS development. These findings may suggest the dependencies on canonical vs non-canonical NF-kB are different in MDS vs AML, as it has been well established that canonical NF-κB signaling plays an important role in AML development (Gasparini et al., 2014; Guzman et al., 2007). In addition, the differential roles of non-canonical NF-κB signaling in MDS and AML may depend on the strength of non-canonical signaling, as the strong constitutive activation of non-canonical signaling via stabilization of NIK in hematopoietic system induces HSPC exhaustion, and bone marrow failure (Xiu et al., 2017), and suppresses MLL-AF9 AML development (Xiu et al., 2018), which is different from chronic inflammatory stimulation in MDS development. These possibilities need to be tested in future studies.

Limitations of the study

There were two limitations to the current study. First, although our data suggest that HOXA9 is differentially regulated by non-canonical (RelB) and canonical (RelA) signaling, the exact mechanism of how TIFAB upregulates HOXA gene program is unclear and will require further investigation in the future. Second, as most of our studies were performed in mouse MLL-AF9 AML cells and human AML cell lines, the result of TIFAB upregulating HOXA genes needs to be validated in human primary AML cells.

STAR★METHODS

Detailed methods are provided in the online version of this paper and include the following:

- KEY RESOURCES TABLE
- RESOURCE AVAILABILITY
  - Lead contact
  - Materials availability
  - Data and code availability
- EXPERIMENTAL MODEL AND SUBJECT DETAILS
- METHOD DETAILS
  - HSPC and LSPC isolation, proliferation and apoptosis analysis
  - BrdU labeling and cell proliferation analysis
  - RNA extraction and quantitative real-time PCR analysis
  - DNA constructs and virus production
  - Western blotting
  - *In vitro* colony-forming assays
  - *In vivo* leukemogenesis
  - Chromatin immunoprecipitation (ChIP)
  - Human *TIFAB* expression analysis
  - RNA-seq and transcriptome analysis
- QUANTIFICATION AND STATISTICAL ANALYSIS

AUTHOR CONTRIBUTIONS

J.M.Z, Y.X., L.F., Q.Z.D, and Y.W. performed the experiments and analyzed the data. N.S.D. and U.K. generated the *Relb*$^{fl/fl}$ line. N.B. assisted with RNA-seq data analysis. B.F.B., and Q.C.L. assisted with data interpretation and manuscript revision. C.Z. conceived and supervised the overall study and wrote the paper.

DECLARATION OF INTERESTS

The authors have no financial interests to declare.

REFERENCES

Bosman, M.C., Schuringa, J.J., and Vellenga, E. (2016). Constitutive NF-kappaB activation in AML: Causes and treatment strategies. Crit. Rev. Oncol. Hematol. *98*, 35–44.

Brunetti, L., Gundry, M.C., Sorcini, D., Guzman, A.G., Huang, Y.H., Ramabadran, R., Gionfriddo, I., Mezzasoma, F., Milano, F., Nabet, B., et al. (2018). Mutant NPM1 maintains the leukemic state through HOX expression. Cancer Cell *34*, 499–512 e499.

Calvo, K.R., Sykes, D.B., Pasillas, M., and Kamps, M.P. (2000). Hoxa9 immortalizes a granulocyte-macrophage colony-stimulating factor-dependent promyelocyte capable of biphenotypic differentiation to neutrophils or macrophages, independent of enforced meis expression. Mol. Cell Biol. *20*, 3274–3285.

Chen, S.L., Qin, Z.Y., Hu, F., Wang, Y., Dai, Y.J., and Liang, Y. (2019). The role of the HOXA gene family in acute myeloid leukemia. Genes (Basel) *10*, 621–632.

Chu, Y., Chen, Y., Li, M., Shi, D., Wang, B., Lian, Y., Cheng, X., Wang, X., Xu, M., Cheng, T., et al. (2019). Six1 regulates leukemia stem cell maintenance in acute myeloid leukemia. Cancer Sci. *110*, 2200–2210.

Collins, C.T., and Hess, J.L. (2016). Role of HOXA9 in leukemia: Dysregulation, cofactors and essential targets. Oncogene *35*, 1090–1098.

De Silva, N.S., Anderson, M.M., Carette, A., Silva, K., Heise, N., Bhagat, G., and Klein, U. (2016). Transcription factors of the alternative NF-kappaB pathway are required for germinal center B-cell development. Proc. Natl. Acad. Sci. U S A *113*, 9063–9068.

Dohner, H., Estey, E., Grimwade, D., Amadori, S., Appelbaum, F.R., Buchner, T., Dombret, H., Ebert, B.L., Fenaux, P., Larson, R.A., et al. (2017). Diagnosis and management of AML in adults: 2017 ELN recommendations from an international expert panel. Blood *129*, 424–447.

Dombret, H., and Gardin, C. (2016). An update of current treatments for adult acute myeloid leukemia. Blood *127*, 53–61.

Farge, T., Saland, E., de Toni, F., Aroua, N., Hosseini, M., Perry, R., Bosc, C., Sugita, M., Stuani, L., Fraisse, M., et al. (2017). Chemotherapy-resistant human acute myeloid leukemia cells are not enriched for leukemic stem cells but require oxidative metabolism. Cancer Discov. *7*, 716–735.

Gasparini, C., Celeghini, C., Monasta, L., and Zauli, G. (2014). NF-kappaB pathways in hematological malignancies. Cell Mol. Life Sci. *71*, 2083–2102.

Guzman, M.L., Rossi, R.M., Neelakantan, S., Li, X., Corbett, C.A., Hassane, D.C., Becker, M.W., Bennett, J.M., Sullivan, E., Lachowicz, J.L., et al. (2007). An orally bioavailable parthenolide analog selectively eradicates acute myelogenous leukemia stem and progenitor cells. Blood *110*, 4427–4435.

Han, S., Li, X., Liang, X., and Zhou, L. (2019). HOXA9 transcriptionally promotes apoptosis and represses autophagy by targeting NF-kappaB in cutaneous squamous cell carcinoma. Cells *8*.

Ito, T., Kwon, H.Y., Zimdahl, B., Congdon, K.L., Blum, J., Lento, W.E., Zhao, C., Lagoo, A., Gerrard, G., Foroni, L., et al. (2010). Regulation of myeloid leukaemia by the cell-fate determinant Musashi. Nature *466*, 765–768.

Jordan, C.T. (2019). Can we selectively target AML stem cells? Best Pract. Res. Clin. Haematol. *32*, 101100.

Jordan, C.T., Guzman, M.L., and Noble, M. (2006). Cancer stem cells. N. Engl. J. Med. *355*, 1253–1261.

Kennedy, V.E., and Smith, C.C. (2020). FLT3 Mutations in acute myeloid leukemia: key concepts and emerging controversies. Front. Oncol. *10*, 612880.

Khwaja, A., Bjorkholm, M., Gale, R.E., Levine, R.L., Jordan, C.T., Ehninger, G., Bloomfield, C.D., Estey, E., Burnett, A., Cornelissen, J.J., et al. (2016). Acute myeloid leukaemia. Nat. Rev. Dis. Primers *2*, 16010.

Kreso, A., and Dick, J.E. (2014). Evolution of the cancer stem cell model. Cell Stem Cell *14*, 275–291.

Kuo, H.P., Wang, Z., Lee, D.F., Iwasaki, M., Duque-Afonso, J., Wong, S.H., Lin, C.H., Figueroa, M.E., Su, J., Lemischka, I.R., et al. (2013). Epigenetic roles of MLL oncoproteins are dependent on NF-kappaB. Cancer Cell *24*, 423–437.

Lagadinou, E.D., Sach, A., Callahan, K., Rossi, R.M., Neering, S.J., Minhajuddin, M., Ashton, J.M., Pei, S., Grose, V., O'Dwyer, K.M., et al. (2013). BCL-2 inhibition targets oxidative phosphorylation and selectively eradicates quiescent human leukemia stem cells. Cell Stem Cell *12*, 329–341.

Love, M.I., Huber, W., and Anders, S. (2014). Moderated estimation of fold change and dispersion for RNA-seq data with DESeq2. Genome Biol. *15*, 550.

Matsumura, T., Kawamura-Tsuzuku, J., Yamamoto, T., Semba, K., and Inoue, J. (2009). TRAF-interacting protein with a forkhead-associated domain B (TIFAB) is a negative regulator of the TRAF6-induced cellular functions. J. Biochem. *146*, 375–381.

Mikkola, H.K., Radu, C.G., and Witte, O.N. (2010). Targeting leukemia stem cells. Nat. Biotechnol. *28*, 237–238.

Milne, T.A., Briggs, S.D., Brock, H.W., Martin, M.E., Gibbs, D., Allis, C.D., and Hess, J.L. (2002). MLL targets SET domain methyltransferase activity to Hox gene promoters. Mol. Cell *10*, 1107–1117.

Mullighan, C.G., Kennedy, A., Zhou, X., Radtke, I., Phillips, L.A., Shurtleff, S.A., and Downing, J.R. (2007). Pediatric acute myeloid leukemia with NPM1 mutations is characterized by a gene expression profile with dysregulated HOX gene expression distinct from MLL-rearranged leukemias. Leukemia *21*, 2000–2009.

Muto, T., Walker, C.S., Choi, K., Hueneman, K., Smith, M.A., Gul, Z., Garcia-Manero, G., Ma, A., Zheng, Y., and Starczynowski, D.T. (2020). Adaptive response to inflammation contributes to sustained myelopoiesis and confers a competitive advantage in myelodysplastic syndrome HSCs. Nat. Immunol. *21*, 535–545.

Niederkorn, M., Agarwal, P., and Starczynowski, D.T. (2020a). TIFA and TIFAB: FHA-domain proteins involved in inflammation, hematopoiesis, and disease. Exp. Hematol. *90*, 18–29.

Niederkorn, M., Hueneman, K., Choi, K., Varney, M.E., Romano, L., Pujato, M.A., Greis, K.D., Inoue, J.I., Meetei, R., and Starczynowski, D.T. (2020b). TIFAB regulates USP15-mediated p53 signaling during stressed and malignant hematopoiesis. Cell Rep. *30*, 2776–2790.e6.

Pai, P., and Sukumar, S. (2020). HOX genes and the NF-kappaB pathway: a convergence of developmental biology, inflammation and cancer biology. Biochim. Biophys. Acta Rev. Cancer *1874*, 188450.

Pollyea, D.A., and Jordan, C.T. (2017). Therapeutic targeting of acute myeloid leukemia stem cells. Blood *129*, 1627–1635.

Subramanian, A., Tamayo, P., Mootha, V.K., Mukherjee, S., Ebert, B.L., Gillette, M.A., Paulovich, A., Pomeroy, S.L., Golub, T.R., Lander, E.S., et al. (2005). Gene set enrichment analysis: a knowledge-based approach for interpreting genome-wide expression profiles. Proc. Natl. Acad. Sci. U S A *102*, 15545–15550.

Tallman, M.S., Wang, E.S., Altman, J.K., Appelbaum, F.R., Bhatt, V.R., Bixby, D., Coutre, S.E., De Lima, M., Fathi, A.T., Fiorella, M., et al. (2019). Acute myeloid leukemia, version 3.2019, NCCN clinical practice guidelines in oncology. J. Natl. Compr. Cancer Netw. *17*, 721–749.

Tang, Z., Li, C., Kang, B., Gao, G., Li, C., and Zhang, Z. (2017). GEPIA: a web server for cancer and normal gene expression profiling and interactive analyses. Nucleic Acids Res. *45*, W98–W102.

Tomczak, K., Czerwinska, P., and Wiznerowicz, M. (2015). The Cancer Genome Atlas (TCGA): an immeasurable source of knowledge. Contemp. Oncol. (Pozn) *19*, A68–A77.

Trivedi, C.M., Patel, R.C., and Patel, C.V. (2008). Differential regulation of HOXA9 expression by nuclear factor kappa B (NF-kappaB) and HOXA9. Gene *408*, 187–195.

Varney, M.E., Niederkorn, M., Konno, H., Matsumura, T., Gohda, J., Yoshida, N., Akiyama, T., Christie, S., Fang, J., Miller, D., et al. (2015). Loss of Tifab, a del(5q) MDS gene, alters hematopoiesis through derepression of Toll-like receptor-TRAF6 signaling. J. Exp. Med. *212*, 1967–1985.

Xiu, Y., Dong, Q., Li, Q., Li, F., Borcherding, N., Zhang, W., Boyce, B., Xue, H.H., and Zhao, C. (2018). Stabilization of NF-kappaB-inducing kinase suppresses MLL-AF9-induced acute myeloid leukemia. Cell Rep. *22*, 350–358.

Xiu, Y., Xu, H., Zhao, C., Li, J., Morita, Y., Yao, Z., Xing, L., and Boyce, B.F. (2014). Chloroquine reduces osteoclastogenesis in murine osteoporosis by preventing TRAF3 degradation. J. Clin. Invest. *124*, 297–310.

Xiu, Y., Xue, W.Y., Lambertz, A., Leidinger, M., Gibson-Corley, K., and Zhao, C. (2017). Constitutive activation of NIK impairs the self-renewal of hematopoietic stem/progenitor cells and induces bone marrow failure. Stem Cells *35*, 777–786.

STAR★METHODS

KEY RESOURCES TABLE

REAGENT or RESOURCE	SOURCE	IDENTIFIER
Antibodies		
BD IMag streptavidin particles Plus-DM	BD Biosciences	#557812
Mouse hematopoietic progenitor (stem) cell enrichment Set-DM	BD Biosciences	#558451
CD117-BV421	BD Biosciences	#562609
Streptavidin PE-CF594	BD Biosciences	#562284
Ki67$^+$ PE	Biolegend	#50-605-860
NF-κB p65 (D14 × 10^{12}) XP(R) rabbit mAb	Cell Signaling Technology	#8242S
p53 (1C12) mouse mAb	Cell Signaling Technology	#2524S
RelB(C1E4) rabbit mAb	Cell Signaling Technology	#4922S
CD16/32-APC	eBioscience	#17-0161-82
CD34-A700	eBioscience	#56-0341-82
Gr-1 PE	eBioscience	#12-5931-83
Mac-1 PE	eBioscience	#12-0112083
Sca1 PE	eBioscience	#12-5981-83
Sca-1 Percp-Cy5.5	eBioscience	#45-5981-82
TIFAB anti-rabbit Antibody	Invitrogen	Prod#PA5-24376
HOXA9 rabbit PolyAb	Proteintech	#I850I-I-AP
β-Actin(C4) mouse clonal IgG	Santa Cruz Biotechnology	Sc-47778
Rabbit immunoglobulin G	Santa Cruz Biotechnology	Sc-2027
Chemicals, peptides, and recombinant proteins		
Cytofix/Cytoperm	BD Biosciences	#554714
SDS-PAGE gels	Bio-Rad	#456-8084
10× RIPA buffer	Cell Signaling Technology	#9806S
Formaldehyde	Cell Signaling Technology	#47746
DMEM	Gibco	#11965-092
RPMI	Gibco	#11875-093
Lipofectamine 3000 Transfection kit	Invitrogen	#L3000-008
Protease inhibitors	Millipore Sigma	11,836,153,001
Mouse FLT3	Peprotech	250-31L
Mouse IL-3 cytokine	Peprotech	213–13
Mouse SCF	Peprotech	250–03
Mouse TPO	Peprotech	315–14
4-OHT	Sigma	SML1666
Tamoxifen	Sigma	T5648
Methocult M3434	Stem Cell Technologies	#03434
In-Fusion® HD Cloning plus	Takara	#638920
Critical commercial assays		
BrdU-APC staining kit	BD Biosciences	#51-9000019AK
PE active Caspase-3 apoptosis kit	BD Biosciences	#550914
iTaq Universal SYBR Green Supermix	Bio-Rad	10,000,068,167

Continued

REAGENT or RESOURCE	SOURCE	IDENTIFIER
SuperScript III first-Strand synthesis SuperMix	Invitrogen	#18080400
NucleoSpin RNA kit	Takara	#740984.50
SMARTer Ultra Low input RNA kit	Takara	#634848
NEBNext Ultra DNA Library Preparation kit	NEB	#E7645S
Deposited data		
Raw and analyzed data	this paper	GEO: GSE178853
Experimental models: Cell lines		
NOMO-1	DSZM	ACC 542
HEK293T	Takara	#632180
Experimental models: Organisms/strains		
NIKΔT3^{flSTOP}	Dr.Klaus Rajewsky	NA
Rosa-CreERT2	Jackson laboratory	stock 008,463
Relb$^{fl/fl}$ mice	Jackson laboratory	stock 028,719
B6 CD45.1	Jackson laboratory	stock 002,014
NIK^{flSTOP}Relb$^{fl/fl}$ERT2	this study	NA
NIKERT2	Xiu et al., 2018	NA
Oligonucleotides		
Hoxa2 forward 5'-TCCCTGGAAATAGCTGATGG-3'; reverse 5'-CCGGTTCTGAAACCACACTT-3'	IDT	NA
Hoxa3 forward 5'-TGTCAAGCCCTTGTCAGAGA-3'; reverse 5'-TGCTGACTGGCATTGTAAGC-3'	IDT	NA
Hoxa5 forward 5'-TTGCGGTCGCTATCCAAATG-3'; reverse 5'-CCATGCCATTGTAGCCGTAG-3'	IDT	NA
Hoxa9 forward 5'-CCGAAAACAATGCCGAGAATG-3'; reverse 5'-GAAACTCCTTCTCCAGTTCCAG-3'	IDT	NA
Hoxa10 forward 5'-GAAAACAGTAAAGCTTCGCCG-3'; reverse 5'-GAAACTCCTTCTCCAGCTCC-3'	IDT	NA
Flt3 forward 5'-ATCATAAGAACAAGCCAGGAGAG-3'; reverse 5'-CATCAGAGGAACAGGACGC-3'	IDT	NA
b-actin forward 5'-AAGGAGATTACTGCTCTGGCTCCTA-3'; reverse 5'-ACTCATCGTACTCCTGCTTGCTGAT-3'	IDT	NA
(CHIP-qPCR) primers for Tifab binding F104 5'-GTCAAGGAAGCCGTACGTAAT-3'; R343 5'-AGGAGAGAAATGGGACAAAGTC-3'; F191 5'-CTACAGTCACGCCTCAACAA-3'; R393 5'-AGTAAGCATTGCCTCTCCAC-3'	IDT	NA
Recombinant DNA		
HOXA9 (murine) FLAG MSCV	Addgene	#8515
pCL-Eco	Addgene	#12371
pMD2.G	Addgene	#12259
psPAX2	Addgene	#12260
pMSCV-IRES-mCherry	Dr. Brian Sorrentino	NA
pLV-IRES-mCherry	Dr. Monica Guzman	NA
Tifab cDNA murine	GenScript	oMu11551
pLV-RELA-IRES-mCherry	this study	NA
pLV-RELB-IRES-mCherry	this study	NA

Continued		
REAGENT or RESOURCE	SOURCE	IDENTIFIER
pMSCV-RelA-IRES-mCherry	Xiu et al., 2018	NA
pMSCV-RelB-IRES-mCherry	Xiu et al., 2018	NA
pMSCV-MLL-AF9-IRES-mCherry	Xiu et al., 2018	NA
Software and algorithms		
DESeq2 v1.30.1	https://genomebiology.biomedcentral.com/articles/10.1186/s13059-014-0550-8	NA
FlowJo (TreeStar)	Flowjo, LLC	https://www.flowjo.com/
Graph Pad Prism (version 5.01)	Graphpad Software	https://www.graphpad.com/
GSEA	https://www.pnas.org/content/102/43/15545	NA
R (version 4.0.5)	https://www.r-project.org/	NA
survival v3.2-11	https://cran.r-project.org/web/packages/survival/index.html	NA
V3.2-11 and survminer v0.4.9	https://cran.r-project.org/web/packages/survminer/index.html	NA

RESOURCE AVAILABILITY

Lead contact

Chen Zhao (cxz545@case.edu).

Materials availability

Plasmids generated in this study are available upon request from the lead contact, Chen Zhao (cxz545@case.edu), but a completed Materials Transfer Agreement may be required.

Data and code availability

- RNA-seq data reported in this paper has been submitted to the GEO archive under accession number GSE178853.

- For each analysis performed, the software and version used have been detailed in the key resources table

- This paper does not report original code.

- Any additional information required to reanalyze the data reported in this paper is available from the lead contact upon request.

EXPERIMENTAL MODEL AND SUBJECT DETAILS

The experiments were conducted under the Institutional Animal Care and Use Committee (IACUC)-approved protocol 2020-0031. Rosa-CreERT2 and NIKERT2 mice (in which mice carrying a NIKΔT3^{flSTOP} allele crossed with Rosa-CreERT2 to conditionally stabilize NIK after Tamoxifen or 4-hydroxytamoxifen (4-OHT) treatment have been described previously (Xiu et al., 2018). Relb$^{fl/fl}$ mice (stock 028,719) (De Silva et al., 2016) and the transplant recipient mice (CD45.1, stock 002,014) were purchased from Jackson Laboratory and crossed with NIKERT2 mice to generate NIK^{flSTOP}Relb$^{fl/fl}$ERT2 mice. All the mouse strains are in a C57BL6 background and were used at 8–12 weeks old with a mix of male and female mice.

METHOD DETAILS

HSPC and LSPC isolation, proliferation and apoptosis analysis

We used the following antibodies from e-Bioscience and BD Biosciences: B220, CD3, CD11b, CD16/32, CD34, CD117, Gr-1, Sca1, and Ter119. For isolation of lineage$^-$c-Kit$^+$Sca-1$^+$ (KLS) cells, whole bone marrow (WBM) cells were incubated with a cocktail of lineage antibodies from BD Biosciences (biotinylated anti-mouse antibodies directed against CD3ε, CD11b, CD45R/B220, Gr-1, Ter119) followed by lineage depletion using BD IMag streptavidin particles Plus-DM, then stained with Sca-1 Percp-Cy5.5, c-kit BV421, and streptavidin PE-CF594. For leukemia cell BrdU incorporation, proliferation (Ki67$^+$), and caspase3/apoptosis

analyses, the following antibodies were used when appropriate: biotinylated lineage markers (CD3, CD4, CD5, CD8, B220, and Ter119) plus streptavidin PE-CF594, Gr-1, Mac-1 and Sca1-PE or PE-Cy5, c-kit-BV421, CD34-A700, CD16/32-APC or -PECy7, BrdU-APC, Ki67-PE, and caspase3-PE. LSRII was used for all the analyses, and FACSAria was used for cell sorting. Data was analyzed using FlowJo (TreeStar).

BrdU labeling and cell proliferation analysis

For *in vitro* BrdU labeling, BrdU was added to culture media to a final concentration of 10 μm. 3 h later, cells were collected and stained first with surface marker (see above), followed by BrdU staining using a BrdU-APC staining kit (BD Biosciences). For Ki67 and caspase3 staining, BM cells were first stained with surface markers to define the progenitor population, followed by fixation and permeabilization with Cytofix/Cytoperm (BD Biosciences) and intracellular staining with Ki67-PE or Caspase3-PE.

RNA extraction and quantitative real-time PCR analysis

RNA was extracted using a NucleoSpin RNA Kit (Takara). Equal amounts of RNA were used for reverse transcriptase reaction, according to the manufacturer's instructions (SuperScript III First-Strand Synthesis SuperMix, Invitrogen). Quantitative PCR (qPCR) was performed with the iTaq Universal SYBR Green Supermix (Bio-Rad). Gene expression levels were normalized to beta-actin. For the primer sequences used, see the key resources table.

DNA constructs and virus production

The plasmids pMSCV-MLL-AF9, pMSCV-RelA-IRES-mCherry and pMSCV-RelB-IRES-mCherry were described previously (Xiu et al., 2018). HOXA9 (murine) FLAG MSCV was a gift from Corey Largman (Addgene plasmid #8515; http://n2t.net/addgene:8515; RRID:Addgene_8515) and pcDNA3.1-C-(k)DYK-TIFAB (murine) was purchased from GenScript and were used as templates for subcloning into BamH1/EcoRI sites of pMSCV-IRES-mCherry using in-fusion following the manufacturer's instructions (Clontech), respectively. RelA and RelB (from MSCV retroviral vectors) were subcloned into pLV-IRES-mCherry (a gift from Dr. Monica Guzman) using in-fusion following the manufacturer's instructions (Clontech). 293T cells were transiently transfected with MSCV vectors with pCL-Eco or pLV vectors with psPAX2 and pMD2.G using lipofectamine 3000 for retrovirus and lentivirus production, respectively.

Western blotting

Leukemia cells were lysed in 1X lysis buffer (10X RIPA Buffer, Cell Signaling Technologies, #9806S) with protease inhibitors. Subsequently, 50 μg of total cellular lysates were loaded in 10% sodium dodecyl sulfate polyacrylamide gel electrophoresis (SDS-PAGE) gels, electro-transferred onto polyvinylidene fluoride (PVDF) membrane and immunoblotted with antibodies to RelA/p65, RelB, NIK, P53 (Cell Signaling Technologies), TIFAB (Invitrogen), HOXA9 (Proteintech), or Beta-actin (Santa Cruz). Membranes were scanned with the ChemiDoc Touch Imaging system (Bio-Rad).

In vitro colony-forming assays

Fluorescence-activated cell sorting (FACS)-sorted (lin⁻c-Kit⁺Sca1⁻CD16⁺CD34⁺) MLL-AF9 leukemia cells were plated (100 cells/24-well plate) in methylcellulose media (Methocult M3434, StemCell Technologies) in the presence or absence of 4-hydroxytamoxifen (4-OHT). Colonies were counted 5–7 days later.

In vivo leukemogenesis

FACS-sorted lineage⁻c-Kit⁺Sca-1⁺ BM cells from NIKERT2, NIKRelb$^{fl/fl}$ERT2, Relb$^{fl/fl}$ or Relb$^{fl/fl}$ERT2 mice were cultured in Dulbecco Modified Eagle Medium supplemented with 10% FBS, 50 ng/mL SCF, 50 ng/mL TPO, 50 ng/mL FLT3 ligand, and 10 ng/mL IL-3 (all from Peprotech, Rocky Hill, NJ) overnight. Then the cells were plated on retrovirus-loaded retronectin-coated plates and spin-infected at 1000 g for 90 min at room temperature and transplanted retro-orbitally into lethally irradiated (950 cGy, single dose) CD45.1 recipient mice (45–100K/recipient) along with 2–3 × 10⁵ rescue cells. 4 weeks post-transplantation, tamoxifen (5 mg/mouse/day, Sigma, St. Louis, MO) was administered daily by oral gavage for 4 days. The leukemia stem/progenitor cells from spleen or BM of primary recipient mice were sorted and transplanted (20,000/recipient) into sublethally (6.5 Gy) irradiated CD45.1 mice. For testing the impact of forced expression of TIFAB and HOXA9, sorted leukemia stem/progenitor cells were infected with vector, TIFAB, or HOXA9 retroviruses, and the infected cells (mCherry⁺) were sorted and then transplanted into sublethally (6.5 Gy) irradiated CD45.1 mice and treated with or without tamoxifen, as described above.

Chromatin immunoprecipitation (ChIP)

ChIP was performed, as described (Xiu et al., 2014). In brief, NIK-stabilized and control primary MLL-AF9 leukemia cells were fixed in 1% formaldehyde. Chromatin was sheared by sonication with a Covaris E220 using the following settings: acoustic duty factor: 5%; peak incident power: 140; cycles per burst: 200; treatment time: 300 s. Sixteen rounds of 20 pulses were made with 2 min between rounds (Qsonica 125 sonicator). Then, samples were incubated overnight at 4°C with Abs to RelB or rabbit immunoglobulin G (IgG) (negative control). Precipitated DNAs were analyzed by real-time PCR. Specific primers for the NF-κB site in the Tifab promoter regions are F104 5′-GTCAAGGAAGCCGTACGTAAT-3′ and R343 5′-AGGAGAGAAATGGGACAAAGTC-3′; F191 5′-CTACAGTCACGCCTCAACAA-3′ and R393 5′-AGTAAG CATTGCCTCTCCAC-3′.

Human *TIFAB* expression analysis

GEPIA2 (Tang et al., 2017) (http://gepia2.cancer-pku.cn/#index) was used to evaluate the mRNA expression of *TIFAB* in AML patients and normal controls. A total of 173 AML patients and 70 normal controls with available *TIFAB* expression data from TCGA (Tomczak et al., 2015) (http://cancergenome.nih.gov) were identified and used for analysis. Of the malignant samples, 167 had overall survival information.

RNA-seq and transcriptome analysis

Total RNA was extracted from sorted LSCs (lin⁻c-kit⁺Sca1⁻CD16⁺CD34⁺) from mice receiving vector- (Con) or TIFAB transduced MLL-AF9 leukemia cells. cDNA synthesis and amplification were performed using the SMARTer Ultra Low Input RNA Kit (Clontech) starting with 20 ng of total RNA per sample, following the manufacturer's instructions. cDNA was fragmented with Q800R sonicator (Qsonica) and used as input for NEBNext Ultra DNA Library Preparation Kit (NEB). Libraries were sequenced on Illumina's HiSeq2000 in single-read mode with a read length of 50 nucleotides producing 60–70 million reads per sample. Sequence data in fastq format were generated using the CASAVA 1.8.2 processing pipeline from Illumina. Differential expression analysis was performed using the DESeq2 v1.30.1 R package (Love et al., 2014). We considered genes differentially expressed between two groups of samples when the DESeq2 analysis resulted in an adjusted p-value of <0.01 and the log2-fold change in gene expression greater than or equal to 1.5 or less than or equal to −1.5. Gene set enrichment analysis (GSEA) was done according to the previous report using the software downloaded from GSEA website (http://software.broadinstitute.org) (Subramanian et al., 2005).

QUANTIFICATION AND STATISTICAL ANALYSIS

Student's t test was used for all but survival curve statistical analyses, and significance was set at $p < 0.05$. Values are means ± standard error of mean (sem). Survival analysis was performed using the survival v3.2-11 and survminer v0.4.9 R packages. For the Kaplan-Meier survival curve, the log rank test was used. Differences with p values < 0.05 were considered significant. *, p < 0.05; **, p < 0.01; ***, p < 0.001.